

Nuclear pre-mRNA Compartmentalization: Trafficking of Released Transcripts to Splicing Factor Reservoirs

Ivo Melčák, Štěpánka Cermanová, Kateřina Jirsová, Karel Koberna, Jan Malínský, and Ivan Raška*

Department of Cell Biology, Institute of Experimental Medicine, Academy of Sciences of Czech Republic, and Laboratory of Gene Expression, Third Medical Faculty, Charles University, 128 00 Prague, Czech Republic

Submitted August 5, 1999; Revised November 9, 1999; Accepted December 15, 1999
Monitoring Editor: Joseph Gall

In the present study, the spatial organization of intron-containing pre-mRNAs of Epstein–Barr virus (EBV) genes relative to location of splicing factors is investigated. The intranuclear position of transcriptionally active EBV genes, as well as of nascent transcripts, is found to be random with respect to the speckled accumulations of splicing factors (SC35 domains) in Namalwa cells, arguing against the concept of the locus-specific organization of mRNA genes with respect to the speckles. Microclusters of splicing factors are, however, frequently superimposed on nascent transcript sites. The transcript environment is a dynamic structure consisting of both nascent and released transcripts, i.e., the track-like transcript environment. Both EBV sequences of the chromosome 1 homologue are usually associated with the track, are transcriptionally active, and exhibit in most cases a polar orientation. In contrast to nascent transcripts (in the form of spots), the association of a post-transcriptional pool of viral pre-mRNA (in the form of tracks) with speckles is not random and is further enhanced in transcriptionally silent cells when splicing factors are sequestered in enlarged accumulations. The transcript environment reflects the intranuclear transport of RNA from the sites of transcription to SC35 domains, as shown by concomitant mapping of DNA, RNA, and splicing factors. No clear vectorial intranuclear trafficking of transcripts from the site of synthesis toward the nuclear envelope for export into the cytoplasm is observed. Using Namalwa and Raji cell lines, a correlation between the level of viral gene transcription and splicing factor accumulation within the viral transcript environment has been observed. This supports a concept that the level of transcription can alter the spatial relationship among intron-containing genes, their transcripts, and speckles attributable to various levels of splicing factors recruited from splicing factor reservoirs. Electron microscopic *in situ* hybridization studies reveal that the released transcripts are directed toward reservoirs of splicing factors organized in clusters of interchromatin granules. Our results point to the bidirectional intranuclear movement of macromolecular complexes between intron-containing genes and splicing factor reservoirs: the recruitment of splicing factors to transcription sites and movement of released transcripts from DNA loci to reservoirs of splicing factors.

INTRODUCTION

Previous results have demonstrated that spliceosome formation and/or splicing can be co-transcriptional (Beyer and Osheim, 1988; LeMaire and Thummel, 1990; Tennyson *et al.*,

1995). In addition, recent results show that transcription and splicing are coupled through interactions of certain factors participating in both of these processes. A large macromolecular complex called “transcriptosome” or “mRNA factory,” containing both transcription and splicing factors, is formed (Corden and Patturajan, 1997; McCracken *et al.*, 1997; Steinmetz, 1997). Polymerase II (pol II) transcriptional and splicing components have been mapped within the cell nucleus. On one hand, they exhibit frequent sites of high local accumulation in the form of microclusters or dots (Neugebauer and Roth, 1997). Such sites likely represent the sites of active transcription and (co-transcriptional) splicing (Neugebauer and Roth, 1997). On the other hand, beside the micro-

* Corresponding author. E-mail address: raskalab@site.cas.cz.
Abbreviations used: AMCA, aminomethylcoumarin; DRB, 5,6-dichloro-1- β -D-ribofuranosylbenzimidazole; EBV, Epstein–Barr virus; EM, electron microscopy; FISH, fluorescence *in situ* hybridization; hnRNP, heterogeneous nuclear ribonucleoprotein; IGC, interchromatin granule cluster; ISH, *in situ* hybridization; NA, numerical aperture; PF, perichromatin fibril; pol II, polymerase II.

clusters, an accumulation of factors of the splicing apparatus is typically mapped to spatially distinct and large domains termed "speckles" (also known as SC35 domains; reviewed in Spector, 1993). These structures are not correlated with RNA pol II transcription (Zeng *et al.*, 1997). It has been shown at the level of activation of some specific unique genes that speckles serve as pools of splicing factors, which are redistributed to the transcription and splicing sites (Misteli *et al.*, 1997).

Although splicing *in vivo* can occur co-transcriptionally, it is not obligatory, because some introns are not removed until after the RNA has been released from the site of synthesis (Zachar *et al.*, 1993; Baurén and Wieslander, 1994; Wuarin and Schibler, 1994). The precise definition of co- and post-transcriptional pre-mRNA distribution is hindered by limited resolution of the stacked structures in conventional light microscopy. Specific pre-mRNA distributions for several genes have been reported, either in the form of local accumulations (spots) or more or less elongated "tracks" (Xing *et al.*, 1993). For the majority of nuclear pre-mRNA accumulations in the form of these tracks, the corresponding active genes are observed to be positioned at or near the periphery of the track, and tracks exhibit polarized configurations with respect to the DNA (Xing and Lawrence, 1993). Using an approach to detect distinct splice-junction sequences, spliced RNAs were found at the site of transcription, pointing to co-transcriptional splicing (Zhang *et al.*, 1994; Huang and Spector, 1996). Furthermore, although some introns were mapped within local RNA accumulations and/or RNA tracks, but closely to the site of synthesis (Kopczynski and Muskavitch, 1992; Xing *et al.*, 1993, 1995; Zhang *et al.*, 1994), other introns were found to be retained within the whole elongated RNA zone (Raap *et al.*, 1991; Lampel *et al.*, 1997; Snaar *et al.*, 1999).

With regard to the spatial relationship of pre-mRNA accumulations relative to speckle domains of splicing factor accumulations, primary transcripts of certain genes as well as the spliced RNAs have been mapped at sites of active transcription and/or outside of speckles (Zhang *et al.*, 1994; Smith *et al.*, 1999). On the other hand, pre-mRNAs from some other genes were shown to be associated (or overlapped) with nuclear speckles (Xing *et al.*, 1993, 1995; Huang and Spector, 1996; Dirks *et al.*, 1997; Ishov *et al.*, 1997; Smith *et al.*, 1999; Snaar *et al.*, 1999). Furthermore, exogenous pre-mRNAs containing a single intron introduced into the nucleus by microinjection exhibited a strong affinity to speckles (Wang *et al.*, 1991). Thus, whether nuclear speckles reflect localized accumulations of active transcription and splicing factors and whether the nucleus is compartmentalized with respect to transcription and splicing remain unresolved.

In the present study, we have addressed the question of whether the transcript environment of intron-containing Epstein-Barr virus (EBV) genes is associated with the speckled organization of splicing factors and whether the organization of splicing factors influences intranuclear transport of RNA within the transcript environment. The EBV system to study pre-mRNA behavior has been chosen for two reasons: 1) viral pre-mRNAs of the different lymphoblastoid cell lines are of similar structure (sequence) but are produced from genomes of different nuclear organization: integrated (Namalwa cells) or episomal (Raji cells); and 2) viral pre-mRNA

is readily detectable under various experimental and methodological conditions because of high expression levels.

This study used fluorescence microscopy, confocal laser scanning microscopy, and electron microscopy (EM) approaches combined with previously described and newly developed techniques to investigate the mutual distribution of genes, RNAs, and splicing factors.

MATERIALS AND METHODS

Cell Lines and Culture

The human lymphoma cell lines Namalwa and Raji were cultured in RPMI-1640 medium (Sigma, St. Louis, MO). Cell culture media were supplemented with 2 mM (RPMI-1640) or 4 mM (Dulbecco's modified Eagle's medium) L-glutamine, 64 µg/ml gentamicin, 0.375% sodium bicarbonate, and 10% FBS (Sigma). Cultures were maintained at 37°C in a 5% CO₂ incubator.

Of the 10 viral genes known to be expressed during EBV latency, 6 encode Epstein-Barr nuclear antigens (EBNAs) (Rogers *et al.*, 1992). They are derived from a long primary transcript by means of alternative splicing and alternative polyadenylation sites (Rogers *et al.*, 1990). All mRNAs have exons in common from the BamHI W viral genomic fragment (the major internal repeat, internal repeat 1). This 3-kb fragment is a sequence reiterated 6–10 times in the EBV genome (Henderson *et al.*, 1983). It was reported for latently infected cell line Namalwa that two copies of 172-kb EBV genomes are integrated in tail-to-tail manner in the single homologue of chromosome 1 and are separated by ~340 kb of cellular DNA (Henderson *et al.*, 1983; Lawrence *et al.*, 1988; Lestou *et al.*, 1996). The Raji cell line harbors between 50 and 100 episomal viral genomes (Delecluse *et al.*, 1993).

In experiments involving transcription inhibitors, cells were incubated with 50 µg/ml 5,6-dichloro-1-β-D-ribofuranosylbenzimidazole (DRB; Calbiochem, La Jolla, CA) or 4 µg/ml actinomycin D (Sigma) and grown for various times before fixation.

Antibodies, DNA Probes, and Constructs

Several antibodies were used in this study: anti-SC35 (Fu and Maniatis, 1990), a gift from X.-D. Fu (University of California, San Diego, CA), 12G4 (Matunis *et al.*, 1992), and 4F4 (Choi and Dreyfuss, 1984), a gift from G. Dreyfuss (University of Pennsylvania Medical School, Philadelphia, PA). A biotin- or digoxigenin-labeled EBV BamHI W probe (Skare and Strominger, 1980) was obtained from J. Lawrence (University of Massachusetts Medical School, Worcester, MA).

In Situ Hybridization

Namalwa and Raji cells were allowed to adhere to gelatin-coated glass coverslips before fixation and further processing for *in situ* hybridization (ISH). For ISH to RNA, the cells were fixed in 4% paraformaldehyde in PBS for 15 min and permeabilized in ascending and descending series of ethanol (50, 75, 95, and 100% ethanol and down, 5 min each) at 4°C. When hybridization to DNA was included, cells were fixed in 4% paraformaldehyde in PBS for 10 min and permeabilized with 0.5% Triton X-100 and 0.5% saponin in PBS for 10 min.

For EM, cells were prefixed in 2% paraformaldehyde in 0.2 M 1,4-piperazinediethanesulfonic acid, pH 6.95, for 10 min and fixed in 8% paraformaldehyde for 4 h. Samples were pelleted in 10% gelatin (Merck, Darmstadt, Germany) in PBS and postfixed for 10 min. The pellets were dehydrated in an ascending series of methanol and then infiltrated and embedded in Lowicryl K4 M resin (Chemische Werke Lowi, Waldkraiburg, Germany) according to a modified progressive lowering of temperature method of Bendayan *et al.* (1987). Ultrathin sections cut on a Reichert Ultracut E ultramicrotome (Leica, Vienna, Austria) were placed on gold EM grids (SCI

Science Services, Munich, Germany). The sections were treated with 1 $\mu\text{g}/\text{ml}$ proteinase K (Boehringer Mannheim, Mannheim, Germany) in 20 mM Tris-HCl, pH 7.4, and 2 mM CaCl_2 at room temperature for 40–45 min. This step greatly increased hybridization efficiency without gross change of the ultrastructure.

Fluorescence in situ hybridization (FISH) was performed as previously described (Lawrence *et al.*, 1989). For each sample 5–10 μl of hybridization mix containing 25–50 ng of probe, 0.5 mg/ml sonicated salmon sperm DNA (Sigma), 2 mg/ml *Escherichia coli* tRNA, 50% deionized formamide, 2 \times SSC, 0.2% BSA, and 20% dextran sulfate was used. The hybridization was done at 37°C in humidified chamber for 3 h to overnight. After posthybridization washes, hybridized probe was detected via primary antibody to biotin (Enzo Biochem, Farmingdale, NY) or digoxigenin (Boehringer Mannheim) and TRITC- or Cy2-conjugated secondary antibodies (Jackson ImmunoResearch, West Grove, PA). To detect DNA sequences, samples were denatured at 72°C for 3 min in 70% deionized formamide and 2 \times SSC and immediately dehydrated through cold ethanol and air dried. For DNA ISH, probes labeled with biotin were used and detected by ExtrAvidin-Cy3 (Sigma). For elimination of RNA, preparations were incubated with 100 $\mu\text{g}/\text{ml}$ RNase A (Boehringer Mannheim) and 200 U/ml RNase H (Sigma) at 37°C for 2 h.

For EM on section ISH, 1.5 μl of hybridization mixture containing 7.5 ng of biotin-labeled probe were used for each grid. ISH was performed at 37°C in a humidified chamber for 80 min. After washing on drops of 50% formamide and 2 \times SSC, pH 7.0, twice for 10 min at 37°C, the grids were rinsed with 4 \times SSC and then PBS using a Pasteur pipette. The sections were preincubated with 0.2% BSA (Sigma) in PBS for 10 min, and the hybridized probe was detected by means of anti-digoxigenin primary antibody (Enzo Biochem) and 6 nm of gold-conjugated secondary antibody (Aurion, Wageningen, The Netherlands). Sections stained with 5% uranyl acetate were examined at 50 kV in an EM 109 transmission electron microscope (Opton Feintech, Oberkochen, Germany).

Combined ISH and Immunocytochemistry

For localization of RNA or DNA sequences relative to SC35 domains, SC35 immunolocalization was performed before ISH. The cells were refixed with 4% paraformaldehyde in PBS for 5 min and processed for hybridization to RNA or DNA. Speckled staining of SC35 was greatly reduced when detected after hybridization. The identical protocol was used for colocalization of heterogeneous nuclear ribonucleoproteins (hnRNPs).

To visualize specific RNA and DNA sequences in the same experiment, a procedure similar to that of Lampel *et al.* (1997) was used. However, instead of two-step image acquisition of relocated cells, this modified protocol does not require cell relocation for the second fluorochrome. Briefly, whole RNA/DNA ISH using a mixture of biotin- and digoxigenin-labeled probes was performed; the probes were initially detected with anti-digoxigenin antibody and Cy2-conjugated secondary antibody. The cells were refixed with 4% paraformaldehyde in PBS for 5 min before RNase digestion of the targeted RNA. The probe hybridized to DNA was detected via ExtrAvidin-Cy3. This method allowed a more precise spatial discrimination between RNA and DNA using differentially labeled probes of the same sequence in a one-step hybridization protocol and in a one-step image acquisition. In this approach, the resolution of the signals is influenced by the optical system only and does not depend on the factor introduced by the investigator.

When appropriate, the cells were counterstained for 5 min in 50 $\mu\text{g}/\text{ml}$ DAPI in PBS and mounted on glass slides in 2.3% (wt/vol) Mowiol 40–88 (Sigma), 42.5% glycerol, and 0.1 M Tris-HCl, pH 8.5, containing 134 mM 1,4-diazabicyclo[2.2.2]octane to reduce fading.

Triple visualization of RNA, DNA, and protein in the same experiment required the consecutive labeling and refixation of the constituents in the order described above. Antibody against SC35 was detected using aminomethylcoumarin acetate (AMCA)-conjugated antibody (Jackson ImmunoResearch).

Cell Spreads and In situ Transcription

Cells adhered onto gelatin-coated glass coverslips were osmotically shrunk with 1 M Tris- PO_4 , pH 9.1, at room temperature for 3.5 min (times shorter than 3 min gave poor spreading). Because of the osmotic shift, the contents of shrunk cells were dispersed rapidly on the surface of the coverslip after placing them into PBS. The structural properties of the cytoplasm are probably the cell type-specific critical parameters for the spreading. In contrast to Namalwa and Raji cells, the cell burst of adherent cells such as HeLa was accompanied by a disruption of intracytoplasmic vacuoles rather than whole-cell spreading (our unpublished results). On the cell spreads, in situ transcription was performed according to the method of Garcia-Blanco *et al.* (1995). Briefly, the spread cells were incubated with transcription mix at 37°C in humidified chamber for 10–15 min. The transcription mix contained 600 μM ATP, GTP, and UTP, 1 mM biotin-14-CTP (Life Technologies, Gaithersburg, MD), 37% buffer D (Dignam *et al.*, 1983), 6.6 mM MgCl_2 , and 10 mM creatine phosphate, supplemented with 37% HeLa nuclear extract (Promega, Madison, WI), enabling downstream EBV transcription of internal repeat 1 *Bam*HI W (van Santen *et al.*, 1983). When visualization of transcription sites by means of brominated uridine was performed, 1 mM 5-bromo-UTP (Sigma) and 600 μM CTP were used. Spreads were fixed in 2% paraformaldehyde in PBS for 10 min and permeabilized in ascending and descending series of ethanol (50, 75, 95, and 100% ethanol and down, 3 min each) at 4°C. Incorporated modified nucleotides were detected via anti-biotin or anti-bromodeoxyuridine (Boehringer Mannheim) primary antibody and TRITC-conjugated secondary antibody (Jackson ImmunoResearch). The sites of incorporation were colocalized with hnRNP K/J proteins using primary antibody 12G4 and Cy2-conjugated secondary antibody. Samples were counterstained for 5 min in 50 $\mu\text{g}/\text{ml}$ DAPI in PBS.

Digital Imaging Microscopy

Confocal Microscopy. Optical sections (0.5 μm) were obtained using a confocal laser scanning microscope (Fluoview; Olympus Optical, Tokyo, Japan; attached to an Olympus BX50 microscope) equipped with a universal plan-apochromat 100/1.35 numerical aperture (NA) objective lens. Fluoview was operated with excitation wavelengths of 488 nm (Cy2 fluorescence) and 568 nm (TRITC/Cy3 fluorescence) from an argon-krypton laser. Fluorescent signals of both fluorochromes were recorded simultaneously by two detectors at one scan.

Fluorescence Microscopy. Samples were examined using an epifluorescence microscope (AX70 Provis; Olympus) fitted with a cooled charge-coupled device camera (PXL; Photometrics, Tucson, AZ) with a Metachrome II coated KAF-1400 chip for extended UV response. Either a universal plan-fluorite 60/1.25 NA or a universal plan-apochromat 100/1.35 NA objective was used. Images were captured using IPLab Spectrum (Signal Analytics, Vienna, VA) software. For dual or triple color labeling, a combination of single-band violet (AMCA), blue (Cy2), and green (TRITC/Cy3) excitors and a triple band-pass emission filter (Chroma Technology, Brattleboro, VT) were used. Images were not subjected to the image restoration algorithm; hence, the signal in the images represents in-focus and out-of-focus fluorescence.

Images were corrected for dark-field current and background. Contrast and opacity were optimized for each channel. Colocalization was performed either by the Fluoview software or by merging the individual channels with IPLab Spectrum.

The images were printed on a Phaser 440 Color Printer (Tektronix, Wilsonville, OR) using Adobe Photoshop (Adobe Systems, Mountain View, CA).

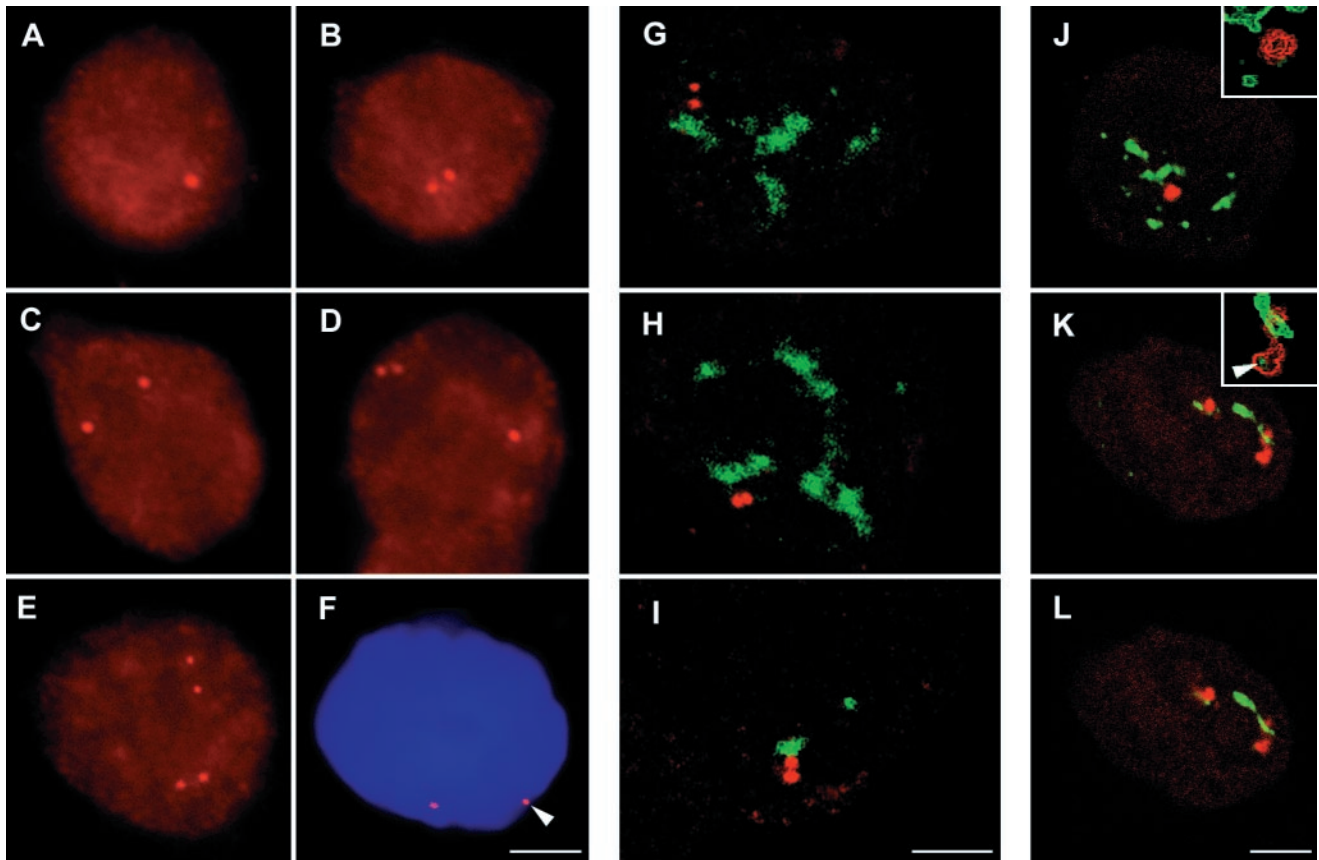


Figure 1. Organization of EBV genomes (A–F) and relationship between SC35 domains and viral DNA (G–I) or RNA (J–L) in Namalwa cells. The pattern of viral genomes distribution in the interphase nuclei of Namalwa cell has been established by DNA FISH of major internal repeat *Bam*HI W. In 34% of cells, a single dot is observed (A). In 48% of cells, two dots closely spaced within the whole range of $\sim 3 \mu\text{m}$ in the x - y plane of each other are observed (B). Seventeen percent of cells have duplicated patterns in three combinations (C–E). A part of the second cell is seen in the bottom part of D. Spatial localization of viral genomes in the interphase nuclei has been performed by means of DNA FISH and DAPI staining; the majority of the signal spatially separated from the nuclear periphery; the minority of genomes have a more peripheral nuclear localization; and some dots are close to nuclear periphery (F, arrowhead). The spatial relationship (documented here by confocal sections) between viral DNA sequences and SC35 domains has been performed by DNA FISH and immunocytochemical mapping by means of the antibody to SC35 splicing factor. In the majority of cells, DNA sequences (red) are observed exclusively outside of the SC35 domains (green; G and I). A smaller fraction of DNA loci, and just one locus in the case of the doublet, is found associated with the outer edge of the SC35 domain (I). Spatial relationship (documented here by confocal sections) between EBV pre-mRNA (red) and SC35 domains (green) has been established by means of RNA FISH and immunocytochemistry. Basically two categories of distribution are observed in the Namalwa cell line. The first category comprises viral RNA spatially separated from SC35 domains (J; the spatial separation is well seen in the inset). The second category includes RNA tightly associated with SC35 domains. This is the major fraction of RNAs forming tracks. RNA signal exhibits various extents of overlap with the SC35 domain (K). The microcluster(s) of SC35 at the pole of RNA accumulations, opposite the SC35 domain, have been observed (K, inset, arrowhead). Insets represent edge-filtered images. K and L are two consecutive confocal sections. Bars, $4.5 \mu\text{m}$.

RESULTS

Organization of EBV Genomes in Namalwa Cells

We visualized EBV genomes by FISH to the *Bam*HI W DNA repeat (Figure 1). Of the 266 analyzed unsynchronized interphasic cells, 48% of the nuclei had two closely spaced spots separated from each other by less than $\sim 3 \mu\text{m}$ (Figure 1B), in agreement with the previous study of Lawrence *et al.* (1989). We termed this pattern of EBV genomes, which apparently represents two spatially resolved viral DNA loci in the chromosome 1 homologue, a doublet. In 34% of cells, a single spot was observed (Figure 1A), which we termed a

singlet. We consider the singlets to be spatially unresolved signals for the two EBV gene loci present in the single chromosome 1 homologue. In the remaining cells, a “duplicated” pattern in three combinations (~ 5 , 6, and 6% of cells; Figure 1, C–E, respectively) was observed, suggesting a subpopulation containing an aneuploid number of chromosome 1 homologue and/or a duplicated chromosome 1 homologue in later phases of the cell cycle. Only a very minor fraction of cells ($\sim 1\%$) exhibited a more complex pattern (our unpublished results), reflecting probably the presence of even more EBV genome copies in interphase nuclei. In all investigated cells it was possible to differentiate between the

category of singlets and doublets on one hand and the category of duplicated or more complex patterns. In this respect, a minimal length threshold (4.5 μm) for a duplicated signal was observed.

The question of viral genome distribution within nuclei was addressed next. The majority of viral genomes were spatially well separated from the nuclear envelope. Only a minority of signal was found within the peripheral nuclear part and/or at the nuclear border (Figure 1F, arrowhead).

Organization of Viral DNA with Respect to SC35 Domains in *Namalwa* Cells

Experiments were performed to address the question of whether there was a specific position of DNA loci relative to speckled domains enriched in SR splicing factors (SC35 domains). The precise dual localization of gene loci and speckles was achieved by a series of consecutive confocal sections. The results showed that DNA loci were randomly distributed with respect to SC35 domains. In the majority of cells, the DNA loci were observed exclusively outside of and spatially separated from the SC35 domains (Figure 1, G and H). A small fraction of DNA loci and usually, in the case of doublets, just one dot of the doublet were found associated with the edge of the SC35 domain (Figure 1I).

Organization of Viral RNA Distributions in *Namalwa* Cells

In ~90% of unsynchronized interphase cells, the viral RNAs were restricted to a well-defined nuclear region. In ~10% of cells, the viral RNA was not detected by ISH. The transcript environment comprised patterns ranging from small spots to track-like regions several micrometers long. From 533 scored cells, the majority (73%) exhibited a single transcript environment. Two transcript environments were very close to each other (distance not exceeding 3 μm in the x-y plane) in 9% of nuclei, often in the form of spots or shorter tracks. Another category of patterns observed in 15% of cells involved spatially well-separated RNA signals. In such a category of signals, the vast majority of cells (14% of total number of scored cells) had two signals separated by several micrometers, and a minor fraction (~1%) showed a combination of two closely spaced signals and a well-separated single accumulation. A small fraction of cells (~2%) exhibited a more complex pattern consisting of multiple signals.

Apparently because of the more localized signal of the gene (one molecule of DNA vs. multiple copies of RNA), the frequency of single RNA environments was, however, much higher with respect to DNA singlets. The single RNA environment thus frequently encompasses the two RNA environments from neighboring genes of the chromosome 1 homologue (also see the next section). The incidence of the RNA patterns is in agreement with the incidence of various DNA patterns (see above).

To investigate whether the position of the transcript environment correlated with the random distribution of their DNA loci relative to SC35 domains, double labeling of viral RNA and splicing factors was performed. It should be noted that the speckled labeling of SC35 was greatly reduced when detected after hybridization (our unpublished results). By confocal microscopy, two categories of distribution were seen. The first category, which comprised a smaller fraction

of RNA signals, consisted of viral RNA environments spatially separated from SC35 domains (Figure 1J). The second category included RNA environments tightly associated with SC35 domains, and it was the major fraction of RNA environments forming tracks. Transcript environments exhibited various extents of overlap with the SC35 domains (Figure 1, K and L).

"Microclusters" (local accumulations) of splicing factors at the pole of RNA accumulations were frequently observed (Figure 1K). These microclusters appeared to be superimposed on the transcript environment. Similar submicrometer microcluster structures of variable size and intensity were seen throughout the nucleoplasm.

Relationship between Viral DNA and RNA in *Namalwa* Cells

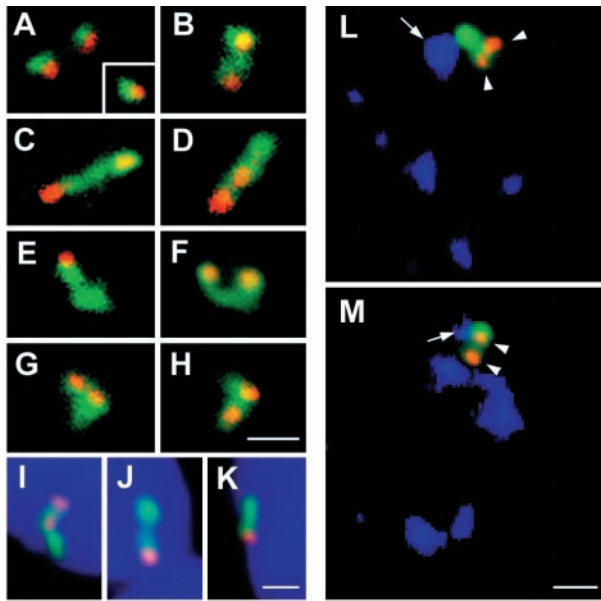
The experiments were performed to address the possibility of a specific position of gene loci relative to transcript environments in *Namalwa* cells. In *Namalwa* cells containing two integrated viral gene copies, a high proportion of the transcript environments are expected to contain two close, spatially well-resolved viral genomes (Lawrence *et al.*, 1988; see Figure 1B).

The specific position of DNA loci was found by dual ISH to both DNA and RNA (Figure 2). We emphasize in this respect that we differentiated the pool of transcripts from the genes by means of visualization of RNA/DNA signal against DNA signal only (see MATERIALS AND METHODS). With respect to the previous approach (Lampel *et al.*, 1997), one-step image acquisition meant a definite methodical improvement.

When RNA/DNA signal was observed in the form of tracks, DNA singlets or doublets were found to be limited to the interior of the track and/or to its periphery (Figure 2, B-H). However, in the majority of tracks, one DNA locus (all loci in the form of singlets and one locus in most cases of doublets) was found at the very extremity of the track (e.g., Figure 2, B-E). In most cases, the DNA loci found at the extremity seemed not to extensively colocalize with RNA/DNA tracks. Importantly, this pattern most likely reflected higher sensitivity and/or resolution of the ExtrAvidin/biotin approach for DNA detection over the RNA/DNA antibody detection of the identical sequence (Lawrence *et al.*, 1989) and was compatible with previous studies (Lawrence *et al.*, 1988, 1990; Trask *et al.*, 1989). Therefore, we identified RNA/DNA tracks with the accumulation of transcripts, i.e., with the RNA signal. No such superimposition position of genes was found at the opposite extremities of any tracks inspected.

When the RNA/DNA signals were just small foci (spots) with no apparent linear axis, the DNA locus was most frequently observed at its periphery (Figure 2A). We interpreted these small RNA accumulations as belonging to the pool of nascent transcripts, whereas tracks encompassed both the nascent and released RNA (see below).

For the minority of RNA accumulations, their outermost parts localized to the nuclear periphery and close to the nuclear envelope (Figure 2, I-K). Some previous studies proposed the view that the RNA accumulation in the form of tracks delineates a path from the gene locus toward the nuclear envelope for its export into the cytoplasm (Lawrence *et al.*, 1989; Dirks *et al.*, 1995; Lampel *et al.*, 1997). However,



the fact that gene loci, together with transcripts, were sometimes localized at the nuclear periphery could also suggest that transcribed RNA occasionally moved inward to the nuclear interior. No clear vectorial route from the DNA locus was observed for the tracks found at the nuclear

Figure 2. Relationship among EBV DNA loci, their transcripts, and SC35 domains in Namalwa cells. The approach exploring DNA FISH, RNA/DNA FISH, immunocytochemistry, and DAPI staining has been used. The spatial relationship between EBV DNA loci and their transcripts is documented in A–H (as well as in I–M). The viral pre-mRNA (green) makes spot or track-like structures of various length (up to several micrometers). With the limit in z-axis resolution in mind, the majority of genes (red) occupy the periphery of the RNA environment. The small RNA accumulation associated with the DNA locus likely represents the pool of nascent transcripts (A and inset). The major fraction of cells exhibit an RNA track, which delineates the path from the gene(s) and encompasses both the nascent and released RNA (B–H). Most tracks are clear-cut polarized with respect to the position of the gene(s), with at least one locus positioned at the extremity of the track (B–E). The polarization of some tracks is less distinct (F–H). Spatial localization of viral DNA (red) and RNA (green) relative to the nuclear periphery (DAPI staining) is documented in I–K. No clear vectorial route from the gene loci to the nuclear envelope could be established. This is well documented in J, in which the track “emanates” from the gene toward the nuclear interior. A part of the second cell is seen in the bottom part of J. In I, the track emanates from the gene toward the nuclear envelope, whereas in K, the track is “parallel” to the nuclear envelope. The relative incidences of tracks seen in J and I are ~40 and 60%, respectively. Simultaneous visualization of viral DNA sequences (red), RNA (green), and SC35 domains (AMCA; blue immunolabeling) is documented in L and M. Tracks encompassing gene loci (arrowheads) emanate toward the SC35 domain (arrow). Bars, 1.5 μm .

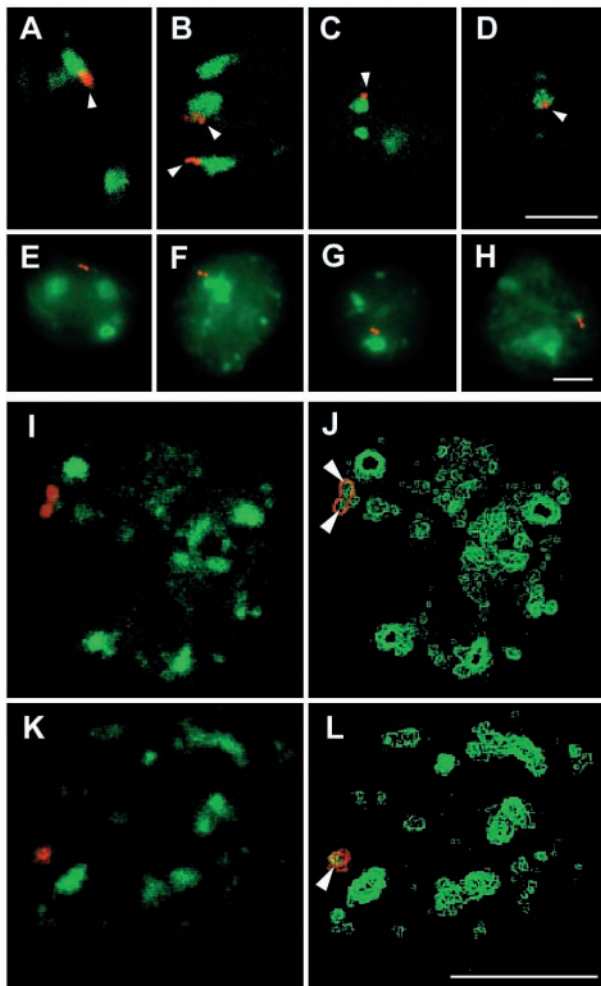


Figure 3. Visualization of the post-transcriptional pool of viral RNA and gene loci in transcriptionally inhibited Namalwa cells and of nascent transcripts in Namalwa cells after resumption of RNA synthesis. Visualization of the post-transcriptional pool of viral RNA (A–D; confocal sections) or gene loci (E–H; conventional fluorescence) and their relationship to SC35 domains is documented. RNA pol II transcription has been inhibited by 50 $\mu\text{g/ml}$ DRB for various periods. The RNA pol II inhibition of transcription caused sequestration of splicing factors in enlarged and rounded-up SC35 domains (green). After 3 h of incubation of cells with DRB, 86% of 93 RNA accumulations (red) are associated with SC35 domains (A and B), and the tracks are generally shorter than in nontreated cells. After an additional 3.5 h of treatment with DRB, the length of the tracks is progressively shortened further, whereas their association with SC35 domains is increased to 96% for the 75 RNA signals analyzed (Figure 3, C and D). However, DNA loci (red) are distributed randomly relative to splicing factor domains within the whole nuclei (Figure 3, E–H). Visualization of nascent viral RNA (red) after a release of cells from the transcriptional block is documented in confocal sections (Figure 3, I–L). The nuclear pool of viral RNA has been depleted by DRB incubation for 13.5 h. The cells were removed from the transcriptional block by replacing the medium and incubated 15 min for recovery. Splicing factors (green) redistributed to a normal speckled pattern (I and K). The vast majority of cells exhibited a single spot (I) or a double spot (3K) of RNA accumulation (red) similar to the gene pattern. RNA spots were spatially separated from the SC35 domains (I and K). The local accumulations of splicing factors (arrowheads) associated with nascent transcripts are seen in the corresponding edge filter images (J and L). Bars: A–K, 6 μm ; I–L, 8 μm .

periphery, and a reverse “movement” of RNA inward to the nuclear interior was indeed observed (Figure 2J).

Relationship among Viral DNA, RNA, and SC35 Domains in Namalwa Cells

We used triple labeling to determine whether a relationship existed between the emergence of transcripts from the gene and the position of the SC35 domain. To simultaneously visualize RNA, DNA, and proteins at the single cell level, an original immunofluorescence ISH (immuno-DNA/RNA ISH) approach based on a consecutive fixation protocol (Xing *et al.*, 1995) was established. The conventional fluorescence microscope was used for the analysis of the triple-labeling experiments, and, on the basis of confocal 3D results on DNA/SC35 mappings, the cells with DNA signals mapped outside of SC35 domains were selected (Figure 2, L and M). In this way we a priori excluded a colocalization of SC35 domains with genes not situated in the focal plane. Our results showed that tracks were polarized both with respect to DNA loci and SC35 domains. The gene(s) was (were) mapped at one extremity of the transcript environments (tracks), whereas the SC35 domain was associated with the opposite part of the track (Figure 2, L and M).

Visualization of the Post-transcriptional Pool of Viral RNA in Namalwa Cells

RNAs in the transcript environment could represent both nascent and finished (released) transcripts. To substantiate a view that released transcripts are directed to SC35 domains, transcription inhibition was used to discriminate viral RNA pools.

RNA pol II transcription was inhibited for various periods with 50 $\mu\text{g}/\text{ml}$ adenosine analogue DRB. DRB, known to interfere with certain serine/threonine protein kinases, notably casein kinase II-type enzymes (Zandomeni *et al.*, 1986; Zandomeni, 1989), has been shown to be a potent carboxyl-terminal domain kinase inhibitor of RNA pol II elongation (Yankulov *et al.*, 1995; Marshall *et al.*, 1996). Several studies have shown that the typical speckled pattern of SR splicing factors is converted into enlarged, round speckles in transcriptionally inactive cells (e.g., O’Keefe *et al.*, 1994).

RNA pol II transcriptional inhibition of Namalwa cells caused sequestration of splicing factors into two to four prominent SC35 domains. Moreover, nucleoplasmic microclusters of splicing factors were observed no more in transcriptionally inhibited cells. Viral RNA was detected in interphase nuclei of DRB-treated Namalwa cells by means of confocal microscopy (Figure 3, A–D). After 3 h of incubation of cells with DRB, 86% of 93 RNA environments were associated with SC35 domains, and the observed RNA tracks were shorter (Figure 3, A and B). After 6.5 h of DRB treatment, the length of the residual transcript environments was progressively shortened further, whereas their association with speckles increased to 96% of the 75 RNA signals analyzed (Figure 3, C and D). On the other hand, DNA loci were distributed randomly and in most cases were not associated with SC35 domains, as shown by conventional microscopy (Figure 3, E–H). The prolonged time of inhibition was accompanied by a decreased number of RNA-positive cells, and viral RNA was not detected in the cells incubated with DRB for 13.5 h (our unpublished results). The association

between viral RNA and SC35 domains was not dependent on continued RNA pol I and III transcription. When cells were treated with actinomycin D at doses (4 $\mu\text{g}/\text{ml}$) that inhibit RNA pol I, II, and III, similar results for RNA signals were obtained (our unpublished results), but the in situ changes occurred after shorter periods, probably because of a rapid uptake of actinomycin D with respect to DRB.

Visualization of the Nascent Pool of Viral RNA in Namalwa Cells

After 13.5 h of DRB treatment, the transcriptional block was removed by replacing the medium, and the cells were incubated 15 min for recovery. Splicing factors became redistributed to the normal speckled pattern (Figure 3, I and K). For the reported RNA pol II elongation rate of ~ 1400 nucleotides/min in vivo (Shermoen and O’Farrell, 1991), the time necessary for the synthesis of the whole primary transcript (Speck and Strominger, 1985; Lawrence *et al.*, 1989) was at least in the range of 30 min. We therefore assumed that after 15 min of incubation time mostly nascent transcripts were being visualized. After resumption of transcription, in cells exhibiting the RNA signal, RNA singlets or doublets similar to the DNA patterns were observed (see Figure 2); i.e., the signals were in the form of spots. Although some RNA spots were found in the vicinity of the SC35 domains, these RNA environments were always spatially separated from the SC35 domains (Figure 3B). Local accumulations of splicing factors, distinct from prominent SC35 domains, were observed at these (nascent) spot-like RNA environments (Figure 3, J and L). After 3 h of incubation, the RNA pattern compatible with that of untreated cells was observed (our unpublished results).

Relationship between Viral RNA and SC35 Domains in Raji Cells

To examine a potentially different pattern, Raji cells were used. In our hands, only a few nuclear RNA spots or tracks per cell were detected in Raji cells. The number was thus far below that we expected based on the number of EBV viral copies present. Whether this reflected clustering of episomes or activity of only some viral copies was not examined.

In 77 analyzed cells, 85% of cells exhibited one to three local RNA accumulations. Three categories of RNA accumulation patterns were observed. As in Namalwa cells, viral RNA was localized either at spatially distinct sites (Figure 4A) or associated with SC35 domains (Figure 4B). Local accumulations of splicing factors at the pole of the RNA environment, distinct from the SC35 domains, were noted (Figure 4, A and B, arrowheads). These local accumulations of splicing factors were more distinct than in Namalwa cells (see Figures 1K and 3, J and L). In contrast to Namalwa cells, RNA environments were often also found inside the SC35 domains (Figure 4C).

RNA Environment Is Enriched in hnRNP K/J Proteins in Namalwa and Raji Cells

Previous studies suggested a possible involvement of hnRNPs in mRNA formation (Dreyfuss *et al.*, 1993). We have analyzed the spatial distribution of several hnRNP proteins relative to viral transcript environment. Although some

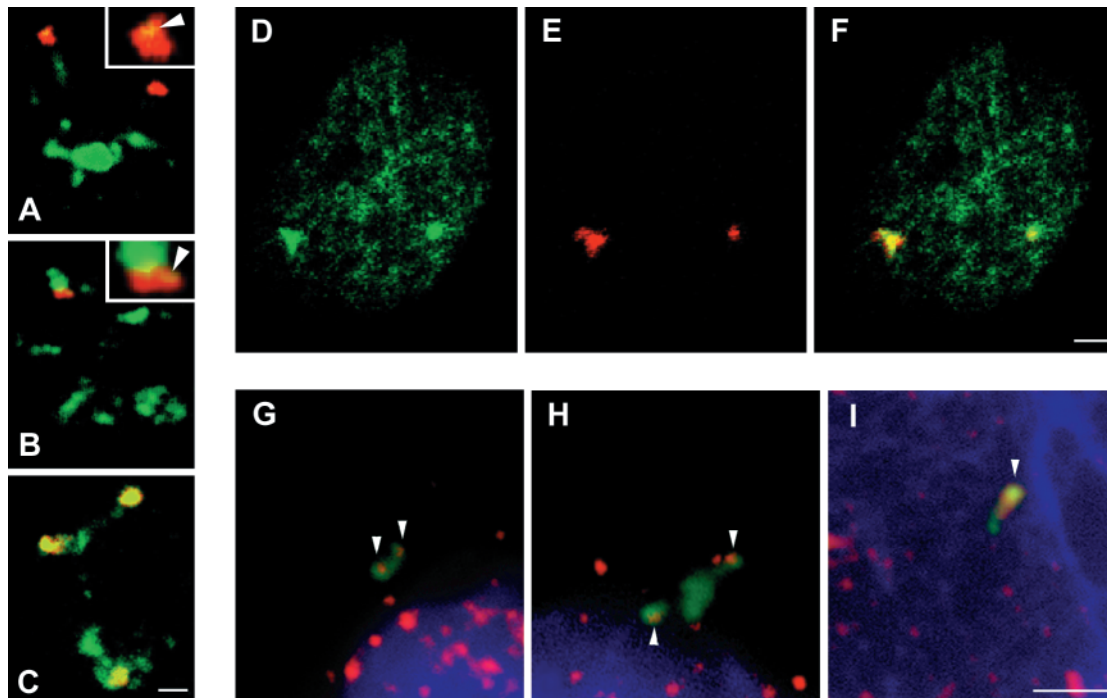


Figure 4. Relationship between viral RNAs and SC35 domains in Raji cells and relationship among viral RNA transcript environment, visualization of nuclear domains enriched in hnRNP K/J proteins, and visualization of transcription sites in the EBV transcript environment (depicted by hnRNP K/J protein immunolabeling). The approach exploring RNA FISH (red) and immunocytochemistry has been used to establish the relationship between viral RNAs and SC35 domains in Raji cells (A–C). In most cells, one to three RNA accumulations are observed. With respect to SC35 domains, RNA signals fall within three categories. As in Namalwa cells, viral RNA is localized as either spatially distinct (A) or associated with SC35 domains (B). However, in contrast to Namalwa cells (see Figure 1), RNA accumulations inside the speckle domains are often found (C). The microclusters of splicing factors distinct from the SC35 domains at the pole of RNA accumulation are clearly visible (insets, arrowheads). By means of RNA FISH and immunocytochemistry, hnRNP K/J proteins (D, green) have been shown to be highly enriched at accumulations of viral RNA (red) in transcriptionally active Raji and Namalwa cells (E). The overlay is documented in F. This fact has been used for the localization of transcription sites at viral RNA accumulations. Visualization of transcription sites (red) in the EBV transcript environment (green) is also shown. Nuclei have been spread by osmotic shift and allowed to transcribe *de novo* in the presence of modified nucleotides. RNA pol II transcriptional competence has been restored by HeLa nuclear extract. Because of a highly diluted nuclear content, single sites of transcription (G–I, red) are easily distinguished. The hnRNP K/J site (K/J site), which colocalizes with the EBV transcript environment (F), is not disrupted by this method (G–I, green). One or two sites of transcription (active genes) are found in the majority of K/J sites of Namalwa spread nuclei (G and H, arrowheads). Sites of transcription colocalize with the K/J site and are of various size, usually much larger in Raji spread cells (I, arrowhead) than in Namalwa cells. Bars, 2 μm.

overlap was observed, hnRNP proteins (e.g., hnRNP C1/C2 proteins) were not enriched in transcript domains (our unpublished results).

In contrast, in addition to its overall nucleoplasmic distribution, high concentrations of hnRNP K/J proteins, which are DNA-binding proteins with transcription factor activity, as well as being hnRNA-binding proteins (Matunis *et al.*, 1992; Takimoto *et al.*, 1993; Michelotti *et al.*, 1996), were observed within the viral RNA environment (Figure 4, D–F). For simplicity, we refer to this distinct nuclear region here as the K/J site.

After transcription inhibition, the residual transcript accumulations still colocalized with the residual, not prominent K/J sites, which were often indistinguishable from the remaining nuclear pool of hnRNP K/J protein (our unpublished results). A reaccumulation of hnRNP K/J proteins into transcript environments required resumption of transcriptional RNA pol II activity (our unpublished results). Thus, disappearance of a prominent K/J site indicates a

depletion of the post-transcriptional pool of viral RNA rather than RNA pol II transcriptional inhibition. In the context of this study, it was not our aim to clarify the reason for the observed accumulation of hnRNP K/J proteins but to use this observation as an immunocytochemical tool in further experiments.

Visualization of Transcription Sites within the Transcript Environment

The massive accumulation of splicing factors within the transcript environment in a subpopulation of Raji cells (Figure 4C) could be considered as a consequence of the splicing factor recruitment to loci of elevated RNA pol II transcriptional activity (Misteli *et al.*, 1997). Because of this, visualization of transcription sites in the viral transcript environment was performed and compared in both Namalwa and Raji cells.

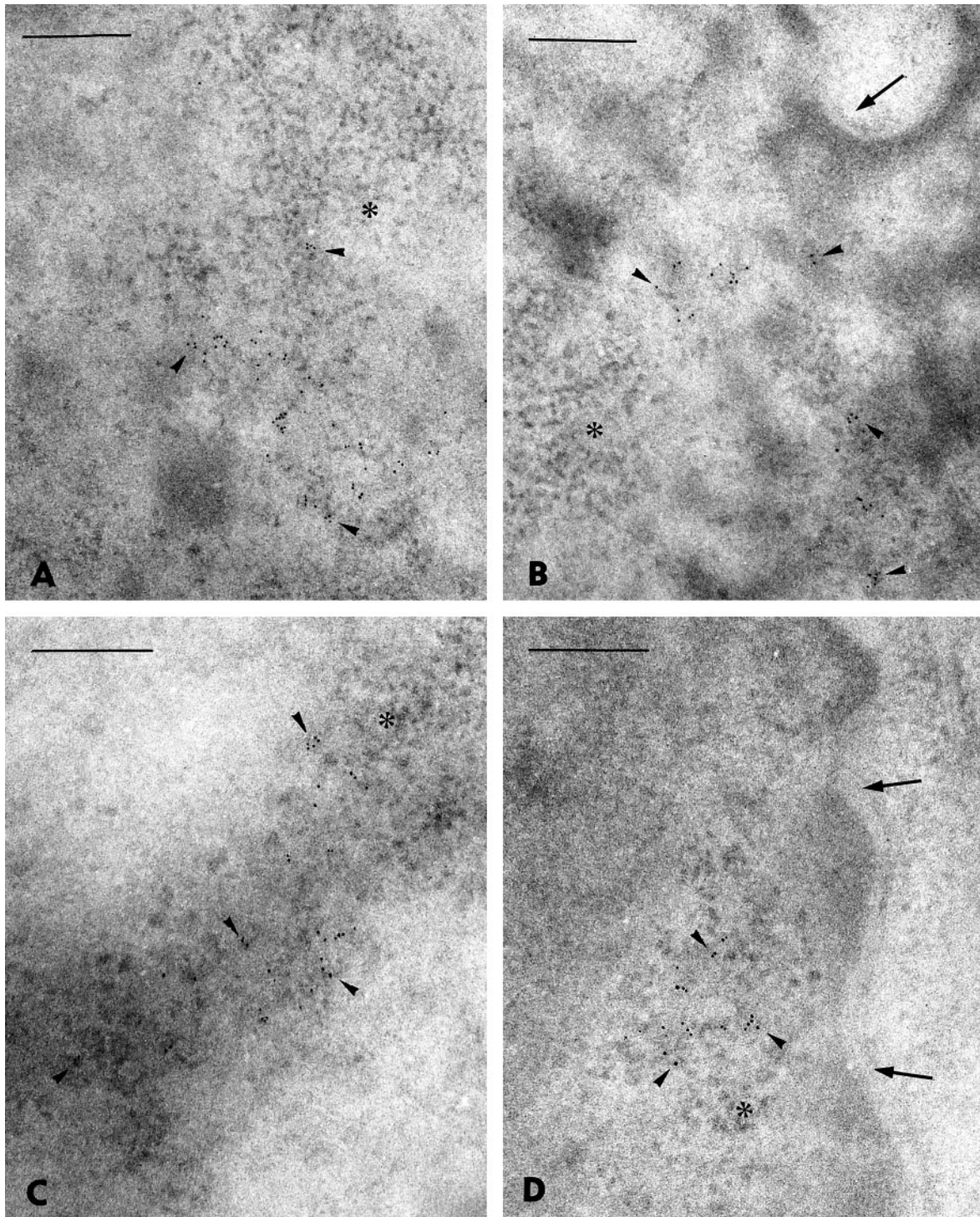


Figure 5. EM localization of viral RNA in nuclei of Namalwa (A and B) and Raji (C and D) cells. By means of postembedding RNA ISH, most of the visualized RNA (6-nm gold particles; arrowheads) are observed in fibrillogranular structures belonging to PFs. A few gold particles (A, C, and D) are found at the border and/or slightly engulfed in clusters of interchromatin granules (asterisk). Note a more pronounced fine structural heterogeneity of PFs observed in Raji cells than in Namalwa cells. For RNA accumulations found at the outermost nuclear region (B and D), the gold particles are not associated with the nuclear envelope (nuclear pores). Bars, 500 nm.

A colocalization of single transcription sites with abundant transcript environment presented a difficulty in interpretation because of a high density of signal, consisting of several hundred to thousands of transcription sites (our unpublished results; Raška, 1995; Iborra *et al.*, 1996; Fay *et al.*, 1997). To be able to identify EBV transcription sites, an approach exploring a spread of nuclear content, similar to that of Garcia-Blanco *et al.* (1995), was used. Moreover, an immunocytochemical approach targeting the hnRNP K/J proteins was chosen for the concomitant visualization of viral RNA, because ISH detection of RNA gave poor results in spread nuclei.

K/J sites were not disrupted by this immunocytochemical method, suggesting the existence of strong structural interactions (Figure 4, G–I). In agreement with results of double RNA/DNA ISH, one or two sites of transcription sites, reflecting the presence of active genes, were found within and/or at the periphery of the majority of K/J sites of spread Namalwa nuclei (Figure 4, G and H). Sites of transcription colocalized with the K/J domain both in Namalwa and Raji cells and were of various sizes. They were usually much larger in Raji (Figure 4I) than in Namalwa (Figure 4, G and H) spread nuclei, and we assumed that K/J sites in Raji cells were associated with loci of higher transcriptional activity than K/J sites in Namalwa cells.

Ultrastructural Description of the RNA Environment

To determine the EM counterpart of the viral transcript environment seen in the light microscope, EM ISH localization of viral RNA in nuclei of Namalwa and Raji cells was performed. Most of the visualized RNA was observed in fibrillogranular structures, which we classified as perichromatin fibrils (PFs) in both Namalwa and Raji cells (Figure 5). This result apparently was documenting different levels of recruitment of splicing factors from their reservoirs organized in interchromatin granule clusters (IGCs) (Misteli *et al.*, 1997), because in contrast to Namalwa cells, the RNA accumulations inside SC35 domains were often found in Raji cells at the light microscopy level. Importantly, a few gold particles were regularly found at the border and/or slightly engulfed in IGCs (Figure 5, A, C, and D), reflecting a physical overlap between the transcript environment and IGCs.

Light microscopy results indicated that the length of the transcript environment is not discriminated by the nuclear envelope (see Figure 2, I–K). The EM results supported this interpretation. RNA accumulations found at the outermost nuclear region (and thus associated with the nuclear envelope at the light microscopy level) were spatially separated from the nuclear envelope (Figure 5, B and D).

DISCUSSION

In the present study, the spatial organization of intron-containing pre-mRNAs of EBV genes relative to location of splicing factors was investigated. Viral pre-mRNA in Namalwa cells and the discriminated pools of nascent and/or finished (released) transcripts were visualized, and their relationship with the organization of splicing factors was established and compared with those in Raji cells.

In transcriptionally active Namalwa cells, the transcript environment was a dynamic structure. It consisted of both nascent and released transcripts, i.e., the track-like transcript environment. Both EBV sequences of the chromosome 1 homologue were usually associated with the track, were transcriptionally active, and exhibited in most cases a polar orientation. In contrast to nascent transcripts (in the form of spots), the association of a post-transcriptional pool of viral pre-mRNA (in the form of tracks) with speckles was not random and was further enhanced in transcriptionally silent cells when splicing factors were sequestered in enlarged accumulations. By means of immuno-DNA/RNA ISH, we have shown that the viral transcript environment reflected the intranuclear transport of RNA from the sites of transcription to SC35 domains.

The appearance of EBV RNA tracks in Namalwa cells has been interpreted as the directed intranuclear trafficking of transcripts from the site of synthesis toward the nuclear envelope for export into the cytoplasm (Lawrence *et al.*, 1989; Dirks *et al.*, 1995; Lampel *et al.*, 1997). Using both light microscopy and EM approaches, no clear vectorial route of EBV RNA toward the nuclear envelope has been observed in the present study. This is consistent with the suggestion of discrete intranuclear steps of RNA transport (Panté *et al.*, 1997). In the fibronectin gene model, which also forms RNA tracks, no clear vectorial route toward the nuclear envelope has been observed, similar to our results (Xing *et al.*, 1993). Our results are in agreement with the concept of trafficking of transcripts to speckles as observed for the directed transport of collagen, human cytomegalovirus immediate early antigen, and β -cardiac myosin heavy chain transcripts to speckles (Xing *et al.*, 1995; Dirks *et al.*, 1997; Ishov *et al.*, 1997; Smith *et al.*, 1999; Snaar *et al.*, 1999).

Importantly, the EBV DNA loci (as well as nascent transcripts) in Namalwa cells were randomly localized with respect to SC35 domains. This unequivocal result argues against the concept of the locus-specific organization of mRNA genes with respect to the speckles (Smith *et al.*, 1999).

Various components of transcription and/or splicing apparatus in mammalian cell nuclei are distributed in a nonuniform manner, i.e., overall nucleoplasmic distribution versus speckles (Spector *et al.*, 1991; Blencowe *et al.*, 1994; Bregman *et al.*, 1995; Sukegawa and Blobel, 1995; Bourquin *et al.*, 1997; Gama-Carvalho *et al.*, 1997; Vyakarnam *et al.*, 1997; Lallena *et al.*, 1998; Mortillaro and Berezney, 1998; Teigelkamp *et al.*, 1998). Despite the fact that the relationship between several actively transcribed genes and the speckles has been established (Xing *et al.*, 1995; Huang and Spector, 1996), the transcription of the whole class of active RNA pol II genes by total uridine incorporation does not rather appear to be correlated with the speckles. It is associated with numerous small nucleoplasmic sites (Fakan and Bernhard, 1971; Fakan and Puvion, 1980; Fakan, 1994; Jackson *et al.*, 1993; Wansink *et al.*, 1993; Fay *et al.*, 1997; Grande *et al.*, 1997; Neugebauer and Roth, 1997; Zeng *et al.*, 1997; Patturajan *et al.*, 1998). Recent results show that transcription and (co-transcriptional) splicing are coupled (Steinmetz, 1997). The evidence has been presented that splicing components colocalize with transcription sites (Neugebauer and Roth, 1997), which supports this idea. In agreement with these data, microclusters of splicing factors in Namalwa cells (as well as in Raji cells) were often found at the extremity of the transcript environment and were distinct from the SC35 domains. This

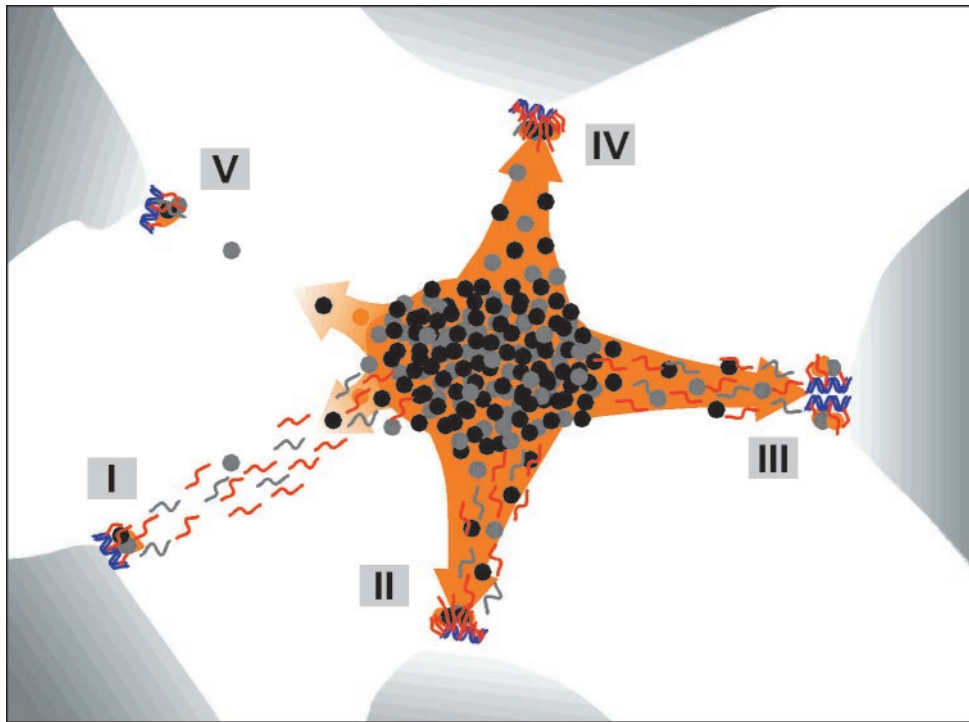


Figure 6. Explanatory sketch of the patterns for genes, transcripts, and splicing factors. Blue helices, genes; red and gray segments, RNA; black, gray, and orange dots, splicing factors; orange area, speckle; orange arrows, recruitment of splicing factors; concentrated dots in the center with the overall ellipsoidal shape, IGC; dots and the gray segments outside of the IGC, PFs. Blue, red, and orange correspond to fluorescence images; EM is in grayscale. (I) Transcription is moderate (or even high), and co-transcriptional splicing is at a low or moderate level. The recruitment of splicing factors is relatively low; much of the unprocessed pre-mRNA is trafficking to IGC. Here, the RNA trafficking clearly prevails over the recruitment of splicing factors, and visualized RNA tracks are associated with the splicing factor reservoirs as observed in Namalwa cells. (II) Example similar to the previous case, but co-transcriptional splicing prevails. There is an elevated recruitment of splicing factors, and (most of) the visualized RNA (RNA tracks) becomes part of the speckle. The corresponding gene becomes associated with the speckle. (III) Example of the local site of high transcriptional activity (depicted here from the clustered genes) and both co- and post-transcriptional splicing. The splicing factors are highly recruited, and both the RNA (as observed in Raji cells) and the genes are extensively engulfed in the speckle. This example is similar to II. (IV) Example of a highly transcribed gene, high recruitment of splicing factors, and co-transcriptional splicing only. Both the RNA (as a spot) and the gene are associated with the speckle. This pattern has been observed rarely in the present study. (V) Example of an endogenous gene expressed at a low level. Transcription is low, as is the recruitment of splicing factors. Visualized RNA appears as a spot at the site of transcription (because of relatively elevated local RNA accumulation), and any directed movement of released RNA is below the level of detection. However, this situation also corresponds to the expressed genes after resumption of RNA synthesis, as seen after DRB treatment of Namalwa cells in this study.

distribution was similar to that of gene loci and was visible particularly well after recovery of Namalwa cells from the transcriptional block at the site of nascent transcripts. These local accumulations disappeared when RNA pol II transcription was shut down and the splicing factors were sequestered to a low number of prominent SC35 domains.

It is a matter of debate whether there is a specific arrangement of intron-containing pre-mRNAs relative to SC35 domains. Previous results indicated that splicing indeed had a spatial relationship with SC35 domains. The detection of specific pre-mRNAs and corresponding spliced mRNAs at the periphery of or within the speckles indicates that these structures are sites of processing for a subset of pre-mRNAs (Huang and Spector, 1991, 1996; Xing *et al.*, 1993, 1995; Ishov *et al.*, 1997; Jolly *et al.*, 1999; Misteli and Spector, 1999; Smith *et al.*, 1999). Several of our results indicate that splicing may have a spatial relationship with SC35 domains: 1) the spatial relationship using simultaneous detection of DNA loci, tran-

scripts, and also splicing factors in unaltered cells indicated that transcript emergence radiated toward the SC35 domain; 2) local accumulations of splicing factors at the sites of nascent transcripts disappeared after transcription block; upon this transcriptional inhibition, the association of viral RNA, most likely representing released transcripts, with SC35 domains was further enhanced; 3) gradual depletion of transcript accumulations, which were associated with SC35 domains, correlated with the duration of transcriptional block; and 4) the normal situation was gradually restored after the release of cells from the transcription block.

We emphasize that, in all these experiments, we do not know whether the visualized RNA undergoes splicing, either before or after it reaches the SC35 domains. However, using the identical model of Namalwa cells, the results of Lampel *et al.* (1997) suggested complete colocalization of intron- and exon-specific probes over the full length of the RNA accumulations without any apparent loss in the inten-

sity of the FISH signal along the track. This indicated that both introns and exons were situated along the entire RNA track. Similar results concerning exon- and intron-specific distribution along the RNA track were reported for the viral human cytomegalovirus immediate early antigen transcripts (Raap *et al.*, 1991; Snaar *et al.*, 1999).

High levels of transcription can alter the apparent spatial relationship between genes and speckles, and the speckle proximity to the gene may thus be a result of dynamic interplay of gene activity and mass action of splicing factors (reviewed in Singer and Green, 1997; also see Xing *et al.*, 1993, 1995; Fakan, 1994; O'Keefe *et al.*, 1994; Pombo *et al.*, 1994; Zhang *et al.*, 1994; Bridge *et al.*, 1996; Huang and Spector, 1996; Fay *et al.*, 1997; Zeng *et al.*, 1997; Aspegren *et al.*, 1998; Misteli *et al.*, 1998). So far, this criterion explains why pre-mRNAs from transfected plasmid DNA with transcription driven from strong promoters, and/or the most abundant endogenous pre-mRNAs, localize in close proximity to and/or within the speckles, whereas transcripts derived from intron-less genes do not lie near speckles (Xing *et al.*, 1993, 1995; Huang and Spector, 1996). The present results with Namalwa and Raji cells are also in harmony with this concept. In comparison with Namalwa cells, transcription signals in Raji cells were more prominent, and RNA environments were also found inside the SC35 domains. Such a dynamic interplay is also documented by distinct differences in the distribution of transcript environments and SC35 domains in nontreated Namalwa cells and those just released from the transcriptional block.

We are of the opinion that the controversy in the interpretation of pre-mRNA distribution relative to the speckled organization of splicing factors depends on the nature of speckles (Huang and Spector, 1996). The speckles have been resolved by EM into two distinct morphological entities, IGCs and PFs (reviewed in Spector *et al.*, 1991; Spector, 1993; Raška, 1995; Huang and Spector, 1996). In this study, distinct differences in the spatial relationship between transcript environments and SC35 domains seen in Namalwa or Raji cells at the light microscope level were expected at the EM level as well. However, basically the same distribution of viral pre-mRNA has been established in both Namalwa and Raji cells by EM. PFs were identified with the most of the viral RNA environment, but viral RNA has been also found distributed in the close association with, or slightly engulfed in, IGCs. From the extensive spatial light microscope analysis of Namalwa cells, the transport of viral RNA from transcription sites to IGCs can thus be inferred.

A concomitant dual mechanism is to be emphasized: an apparent recruitment of splicing factors to transcription sites (Huang and Spector, 1996; Misteli *et al.*, 1997) in both Namalwa and Raji cells on one hand and the association of the released transcripts with the reservoirs of splicing factors on the other (Figure 6). The speckles primarily correspond to IGCs, i.e., to the reservoirs of splicing factors. In the case of highly active genes, as documented in the present study, the speckles correspond both to IGCs and PFs. The association of a track-like transcript environment with the speckle reflects that the extent of trafficking of released transcripts to splicing factor reservoirs (IGCs) prevails. The overlap of the same transcript environment with the speckle reflects an elevated gene activity and an increased recruitment of splicing factors to sites of RNA synthesis, resulting in the over-

shadowing of transcript transport by extensive colocalization of transcripts and splicing factors.

Not all pre-mRNA sequences are processed co-transcriptionally, and post-transcriptional splicing does occur (Zachar *et al.*, 1993; Baurén and Wieslander, 1994; Wuarin and Schibler, 1994). We proposed earlier that unspliced transcripts, which skip co-transcriptional splicing, are called on as needed and released from the site of synthesis by mass action to the speckles (Melčák and Raška, 1996). The reservoir of splicing factors may facilitate post-transcriptional processing. We believe that both splicing factors associated with nascent transcripts seen as local accumulations of splicing factors (recruited splicing factors) sensitive to transcription inhibition and splicing factors stalled in the reservoirs (IGCs) are two functionally related structures. The first may reflect co-transcriptional splicing, whereas the latter may reflect mostly post-transcriptional splicing, which does not depend on the ongoing transcription.

ACKNOWLEDGMENTS

We thank J. Lawrence for interest in and encouragement of this work. Antibodies and labeled DNA probes were kindly supplied by X.-D. Fu (anti-SC35), G. Dreyfuss (12G4 and 4F4 antibodies), and J. Lawrence (EBV *BamHI* W probes). We are also grateful to J. McNeil for advice on ISH, J. Reischig for access to the confocal microscope, Václava Rohlenová for help with preparation of figures, and K. Raska, Jr., for review of the manuscript. This work was supported by Wellcome grant 049949/Z/97/Z/JMW/JPS/CG, Grant Agency of the Czech Republic research grants 302/99/0587 and 304/00/1481, and Ministry of Education, Youth and Sports research grant VS 96129. Results of this work have been presented at the Cold Spring Harbor Laboratory Meeting on the Dynamic Organization of Nuclear Function, Cold Spring Harbor, NY, October 7–11, 1998, and the European Molecular Biology Organization Workshop on the Functional Organization of the Cell Nucleus, Prague, August 9–12, 1999.

REFERENCES

- Aspegren, A., Rabino, C., and Bridge, E. (1998). Organization of splicing factors in adenovirus-infected cells reflects changes in gene expression during the early to late phase transition. *Exp. Cell Res.* 245, 203–213.
- Baurén, G., and Wieslander, L. (1994). Splicing of Balbiani ring 1 gene pre-mRNA occurs simultaneously with transcription. *Cell* 76, 183–192.
- Bendayan, M., Nanci, A., and Kan, F.W.K. (1987). Effect of tissue processing on colloidal gold cytochemistry. *J. Histochem. Cytochem.* 35, 983–996.
- Beyer, A.L., and Osheim, Y.N. (1988). Splice site selection, rate of splicing, and alternative splicing on nascent transcripts. *Genes Dev.* 2, 754–765.
- Blencowe, B.J., Nickerson, J.A., Issner, R., Penman, S., and Sharp, P.A. (1994). Association of nuclear matrix antigens with exon-containing splicing complexes. *J. Cell Biol.* 127, 593–607.
- Bourquin, J.P., Stagljar, I., Meier, P., Moosmann, P., Silke, J., Baechli, T., Georgiev, O., and Schaffner, W. (1997). A serine/arginine-rich nuclear matrix cyclophilin interacts with the C-terminal domain of RNA polymerase II. *Nucleic Acids Res.* 25, 2055–2061.
- Bregman, D.B., Du, L., van der Zee, S., and Warren, S.L. (1995). Transcription-dependent redistribution of the large subunit of RNA polymerase II to discrete nuclear domains. *J. Cell Biol.* 129, 287–298.

- Bridge, E., Riedel, K.U., Johansson, B.M., and Pettersson, U. (1996). Spliced exons of adenovirus late RNAs colocalize with snRNP in a specific nuclear domain. *J. Cell Biol.* *135*, 303–314.
- Choi, Y.D., and Dreyfuss, G. (1984). Monoclonal antibody characterization of the C proteins of heterogeneous nuclear ribonucleoprotein complexes in vertebrate cell. *J. Cell Biol.* *99*, 1997–2004.
- Corden, J.L., and Patturajan, M. (1997). A CTD function linking transcription to splicing. *Trends Biochem. Sci.* *22*, 413–416.
- Decluse, H.J., Barnizke, S., Hammerschmidt, W., Bullerdiek, J., and Bornkamm, G.W. (1993). Episomal and integrated copies of Epstein-Barr virus coexist in Burkitt lymphoma cell lines. *J. Virol.* *67*, 1292–1299.
- Digham J.D., Lebovitz, R.M., and Roedor, R.G. (1983). Accurate transcription initiation by RNA polymerase II in a soluble extract from isolated mammalian nuclei. *Nucleic Acids Res.* *11*, 1475–1489.
- Dirks, R.W., Daniel, K.C., and Raap, A.K. (1995). RNAs radiate from gene to cytoplasm as revealed by fluorescence in situ hybridization. *J. Cell Sci.* *108*, 2565–2572.
- Dirks, R.W., de Pauw, E.S., and Raap, A.K. (1997). Splicing factors associate with nuclear HCMV-IE transcripts after transcriptional activation of the gene, but dissociate upon transcription inhibition: evidence for a dynamic organization of splicing factors. *J. Cell Sci.* *110*, 515–522.
- Dreyfuss, G., Matunis, M.J., Pinol-Roma, S., and Burd, C.G. (1993). hnRNP proteins and the biogenesis of mRNA. *Annu. Rev. Biochem.* *62*, 289–321.
- Fakan, S. (1994). Perichromatin fibrils are in situ forms of nascent transcripts. *Trends Cell Biol.* *4*, 86–90.
- Fakan, S., and Bernhard, W. (1971). Localization of rapidly and slowly labeled nuclear RNA as visualized by high resolution autoradiography. *Exp. Cell Res.* *67*, 129–141.
- Fakan, S., and Puvion, E. (1980). The ultrastructural visualization of nucleolar and extranucleolar RNA synthesis and distribution. *Int. Rev. Cytol.* *65*, 255–299.
- Fay, F.S., Taneja, K.L., Shenoy, S., Lifshitz, L., and Singer, R.H. (1997). Quantitative digital analysis of diffuse and concentrated nuclear distributions of nascent transcripts, SC35 and poly(A). *Exp. Cell Res.* *231*, 27–37.
- Fu, X.D., and Maniatis, T. (1990). Factor required for mammalian spliceosome assembly is localized to discrete regions in the nucleus. *Nature* *343*, 437–441.
- Gama-Carvalho, M., Krauss, R.D., Chiang, L., Valcárcel, J., Green, M.R., and Carmo-Fonseca, M. (1997). Targeting of U2AF65 to sites of active splicing in the nucleus. *J. Cell Biol.* *137*, 975–987.
- Garcia-Blanco, M.A., Miller, D.D., and Sheetz, M.P. (1995). Nuclear spreads: I. Visualization of bipartite rRNA domains. *J. Cell Biol.* *128*, 15–27.
- Grande, M.A., van der Kraan, I., de Jong, L., and van Driel, R. (1997). Nuclear distribution of transcription factors in relation to sites of transcription and RNA polymerase II. *J. Cell Sci.* *110*, 1781–1791.
- Henderson, A., Ripley, S., Heller, M., and Kieff, E. (1983). Chromosome site for Epstein-Barr virus DNA in a Burkitt tumor cell line and in lymphocytes growth-transformed in vitro. *Proc. Natl. Acad. Sci. USA* *80*, 1987–1991.
- Huang, S., and Spector, D.L. (1991). Nascent pre-mRNA transcripts are associated with nuclear regions enriched in splicing factors. *Genes Dev.* *5*, 2288–2302.
- Huang, S., and Spector, D.L. (1996). Intron-dependent recruitment of pre-mRNA splicing factors to sites of transcription. *J. Cell Biol.* *133*, 719–732.
- Iborra, F.J., Pombo, A., Jackson, D.A., and Cook, P.R. (1996). Active RNA polymerases are localized within discrete transcription “factories” in human nuclei. *J. Cell Sci.* *109*, 1427–1436.
- Ishov, A.M., Stenberg, R.M., and Maul, G.G. (1997). Human cytomegalovirus immediate early interaction with host nuclear structures: definition of an immediate transcript environment. *J. Cell Biol.* *138*, 5–16.
- Jackson, D.A., Hassan, A.B., Errington, R.J., and Cook, P.R. (1993). Visualization of focal sites of transcription within human nuclei. *EMBO J.* *12*, 1059–1065.
- Jolly, C., Vourc’h, C., Robert-Nicoud, M., and Morimoto, R.I. (1999). Intron-dependent association of splicing factors with active genes. *J. Cell Biol.* *145*, 1133–1143.
- Kopczynski, C.C., and Muskavitch, M.A. (1992). Introns excised from the Delta primary transcript are localized near sites of Delta transcription. *J. Cell Biol.* *119*, 503–512.
- Lallena, M.J., Martinez, C., Valcárcel, J., and Correas, I. (1998). Functional association of nuclear protein 4.1 with pre-mRNA splicing factors. *J. Cell Sci.* *111*, 1963–1971.
- Lampel, S., Bridger, J.M., Zirbel, R.M., Mathieu, U.R., and Lichter, P. (1997). Nuclear RNA accumulations contain released transcripts and exhibit specific distributions with respect to Sm antigen foci. *DNA Cell Biol.* *16*, 1133–1142.
- Lawrence, J.B., Singer, R.H., and Marselle, L.M. (1989). Highly localized tracks of specific transcripts within interphase nuclei visualized by in situ hybridization. *Cell* *57*, 493–502.
- Lawrence, J.B., Singer, R.H., and McNeil, J.A. (1990). Interphase and metaphase resolution of different distances within the human dystrophin gene. *Science* *249*, 928–932.
- Lawrence, J.B., Villave, C.A., and Singer, R.H. (1988). Sensitive, high-resolution chromatin and chromosome mapping in situ: presence and orientation of two closely integrated copies of EBV in a lymphoma line. *Cell* *52*, 51–61.
- LeMaire, M.F., and Thummel, C.S. (1990). Splicing precedes polyadenylation during *Drosophila* E74A transcription. *Mol. Cell Biol.* *10*, 6059–6063.
- Lestou, V.S., Strehl, S., Lion, T., Gadner, H., and Ambros, P.F. (1996). High-resolution FISH of the entire integrated Epstein-Barr virus genome on extended human DNA. *Cytogenet. Cell Genet.* *74*, 211–217.
- Marshall, N.F., Peng, J., Xie, Z., and Price, D.H. (1996). Control of RNA polymerase II elongation potential by a novel carboxyl-terminal domain kinase. *J. Biol. Chem.* *271*, 27176–27183.
- Matunis, M.J., Michael, W.M., and Dreyfuss, G. (1992). Characterization and primary structure of the poly(C)-binding heterogeneous nuclear ribonucleoprotein complex K protein. *Mol. Cell Biol.* *12*, 164–171.
- McCracken, S., Fong, N., Yankulov, K., Ballantyne, S., Pan, G., Greenblatt, J., Patterson, S.D., Wickens, M., and Bentley, D.L. (1997). The C-terminal domain of RNA polymerase II couples mRNA processing to transcription. *Nature* *385*, 357–361.
- Melčák, I., and Raška, I. (1996). Structural organization of the pre-mRNA splicing commitment. A hypothesis. *J. Struct. Biol.* *117*, 189–194.
- Michelotti, E.F., Michelotti, G.A., Aronsohn, A.I., and Levens, D. (1996). Heterogenous nuclear ribonucleoprotein K is a transcription factor. *Mol. Cell Biol.* *16*, 2350–2360.
- Misteli, T., Cáceres, J.F., Clement, J.Q., Krainer, A.R., Wilkinson, M.F., and Spector, D.L. (1998). Serine phosphorylation of SR proteins is required for their recruitment to sites of transcription in vivo. *J. Cell Biol.* *143*, 297–307.
- Misteli, T., Cáceres, J.F., and Spector, D.L. (1997). The dynamics of a pre-mRNA splicing factor in living cells. *Nature* *387*, 523–527.

- Misteli, T., and Spector, D.L. (1999). RNA polymerase II targets pre-mRNA splicing factors to transcription sites in vivo. *Mol. Cell* 3, 697–705.
- Mortillaro, M.J., and Berezney, R. (1998). MatrIn CYP, an SR-rich cyclophilin that associates with the nuclear matrix and splicing factors. *J. Biol. Chem.* 273, 8183–8192.
- Neugebauer, K.M., and Roth, M.B. (1997). Distribution of pre-mRNA splicing factors at sites of RNA polymerase II transcription. *Genes Dev.* 11, 1148–1159.
- O’Keefe, R.T., Mayeda, A., Sadowski, C.L., Krainer, A.R., and Spector, D.L. (1994). Disruption of pre-mRNA splicing in vivo results in reorganization of splicing factors. *J. Cell Biol.* 124, 249–260.
- Panté, N., Jarmolowski, A., Izaurralde, E., Sauder, U., Baschong, W., and Mattaj, I.W. (1997). Visualizing nuclear export of different classes of RNA by electron microscopy. *RNA* 3, 498–513.
- Patturajan, M., Wei, X., Berezney, R., and Corden, J.L. (1998). A nuclear matrix protein interacts with the phosphorylated C-terminal domain of RNA polymerase II. *Mol. Cell Biol.* 18, 2406–2415.
- Pombo, A., Ferreira, J., Bridge, E., and Carmo-Fonseca, M. (1994). Adenovirus replication and transcription sites are spatially separated in the nucleus of infected cells. *EMBO J.* 13, 5075–5085.
- Raap, A.K., van de Rijke, F.M., Dirks, R.W., Sol, C.J., Boom, R., and van der Ploeg, M. (1991). Bicolor fluorescence in situ hybridization to intron and exon mRNA sequences. *Exp. Cell Res.* 197, 319–322.
- Raška, I. (1995). Nuclear ultrastructures associated with the RNA synthesis and processing. *J. Cell. Biochem.* 59, 11–26.
- Rogers, R.P., Strominger, J.L., and Speck, S.H. (1992). Epstein-Barr virus in B lymphocytes: viral gene expression and function in latency. *Adv. Cancer Res.* 58, 1–26.
- Rogers, R.P., Woisetschlaeger, M., and Speck, S.H. (1990). Alternative splicing dictates translational start in Epstein-Barr virus transcripts. *EMBO J.* 9, 2273–2277.
- Shermoen, A.W., and O’Farrell, P.H. (1991). Progression of the cell cycle through mitosis leads to abortion of nascent transcripts. *Cell* 67, 303–310.
- Singer, R.H., and Green, M.R. (1997). Compartmentalization of eukaryotic gene expression: causes and effects. *Cell* 91, 291–294.
- Skare, J., and Strominger, J. (1980). Cloning and mapping of *Bam*HI endonuclease fragments of DNA from the transforming B95–8 strain of Epstein-Barr virus. *Proc. Natl. Acad. Sci. USA* 77, 3860–3864.
- Smith, K.P., Moen, P.T., Wydner, K.L., Coleman, J.R., and Lawrence, J.B. (1999). Processing of endogenous pre-mRNAs in association with SC-35 domains is gene specific. *J. Cell Biol.* 144, 617–629.
- Snaar, S.P., Vincent, M., and Dirks, R.W. (1999). RNA polymerase II localizes at sites of human cytomegalovirus immediate-early RNA synthesis and processing. *J. Histochem. Cytochem.* 47, 245–254.
- Speck, S.H., and Strominger, J.L. (1985). Analysis of the transcript encoding the latent Epstein-Barr virus nuclear antigen I: a potentially polycistronic message generated by long-range splicing of several exons. *Proc. Natl. Acad. Sci. USA* 82, 8305–8309.
- Spector, D.L. (1993). Nuclear organization of pre-mRNA processing. *Curr. Opin. Cell Biol.* 5, 442–448.
- Spector, D.L., Fu, X.D., and Maniatis, T. (1991). Associations between distinct pre-mRNA splicing components and the cell nucleus. *EMBO J.* 10, 3467–3481.
- Steinmetz, E.J. (1997). Pre-mRNA processing and the CTD of RNA polymerase II: the tail that wags the dog? *Cell* 89, 491–494.
- Sukegawa, J., and Blobel, G. (1995). A putative mammalian RNA helicase with an arginine-serine-rich domain colocalizes with a splicing factor. *J. Biol. Chem.* 270, 15702–15706.
- Takimoto, M., Tomonaga, T., Matunis, M., Avigan, M., Krutzsch, H., Dreyfuss, G., and Levens, D. (1993). Specific binding of heterogeneous ribonucleoprotein particle protein K to the human c-myc promoter, in vitro. *J. Biol. Chem.* 268, 18249–18258.
- Teigelkamp, S., Achsel, T., Mundt, C., Gotherl, S.F., Cronshagen, U., Lane, W.S., Marahiel, M., and Luhrmann, R. (1998). The 20 kDa protein of human [U4/U6.U5] tri-snRNPs is a novel cyclophilin that forms a complex with the U4/U6-specific 60 kDa and 90 kDa proteins. *RNA* 4, 127–141.
- Tennyson, C.N., Klamut, H.J., and Worton, R.G. (1995). The human dystrophin gene requires 16 h to be transcribed and is cotranscriptionally spliced. *Nat. Genet.* 9, 184–190.
- Trask, B., Pinkel, D., and Van den Engh, G. (1989). The proximity of DNA sequences in interphase cell nuclei is correlated to genomic distance and permits ordering of cosmids spanning 250 kb pairs. *Genomics* 5, 710–717.
- van Santen, V., Cheung, A., Hummel, M., and Kieff, E. (1983). RNA encoded by the IR1–U2 region of Epstein-Barr virus DNA in latently infected, growth-transformed cells. *J. Virol.* 46, 424–433.
- Vyakarnam, A., Dagher, S.F., Wang, J.L., and Patterson, R.J. (1997). Evidence for a role for galectin-1 in pre-mRNA splicing. *Mol. Cell Biol.* 17, 4730–4737.
- Wang, J., Cao, L.G., Wang, Y.L., and Pederson, T. (1991). Localization of pre-messenger RNA at discrete nuclear sites. *Proc. Natl. Acad. Sci. USA* 88, 7391–7395.
- Wansink, D.G., Schul, W., van der Kraan, I., van Steensel, B., van Driel, R., and de Jong, L. (1993). Fluorescent labeling of nascent RNA reveals transcription by RNA polymerase II in domains scattered throughout the nucleus. *J. Cell Biol.* 122, 283–293.
- Wuarin, J., and Schibler, U. (1994). Physical isolation of nascent RNA chains transcribed by RNA polymerase II: evidence for cotranscriptional splicing. *Mol. Cell Biol.* 14, 7219–7225.
- Xing, Y., Johnson, C.V., Dobner, P., and Lawrence, J.B. (1993). Higher level organization of individual gene transcription and RNA splicing: integration of nuclear structure and function. *Science* 259, 1326–1330.
- Xing, Y., Johnson, C.V., Moen, P.T., Jr., McNeil, J.A., and Lawrence, J.B. (1995). Nonrandom gene organization: structural arrangements of specific pre-mRNA transcription and splicing with SC-35 domains. *J. Cell Biol.* 131, 1635–1647.
- Xing, Y., and Lawrence, J.B. (1993). Nuclear RNA tracks: structural basis for transcription and splicing? *Trends Cell Biol.* 3, 346–353.
- Yankulov, K., Yamashita, K., Roy, R., Egly, J.M., and Bentley, D.L. (1995). The transcriptional elongation inhibitor 5,6-dichloro-1- β -D-ribofuranosylbenzimidazole inhibits transcription factor IIIH-associated protein kinase. *J. Biol. Chem.* 270, 23922–23925.
- Zachar, Z., Kramer, J., Mims, I.P., and Bingham, P.M. (1993). Evidence for channeled diffusion of pre-mRNAs during nuclear RNA transport in metazoans. *J. Cell Biol.* 121, 729–742.
- Zandomeni, R., Zandomeni, M.C., Shugar, D., and Weinmann, R. (1986). Casein kinase type II is involved in the inhibition by 5,6-dichloro-1- β -D-ribofuranosylbenzimidazole of specific RNA polymerase II transcription. *J. Biol. Chem.* 261, 3414–3419.
- Zandomeni, R.O. (1989). Kinetics of inhibition by 5,6-dichloro-1- β -D-ribofuranosylbenzimidazole on calf thymus casein kinase II. *Biochem. J.* 262, 469–473.
- Zeng, C., Kim, E., Warren, S.L., and Berget, S.M. (1997). Dynamic relocation of transcription and splicing factors dependent upon transcriptional activity. *EMBO J.* 16, 1401–1412.
- Zhang, G., Taneja, K.L., Singer, R.H., and Green, M.R. (1994). Localization of pre-mRNA splicing in mammalian nuclei. *Nature* 372, 809–812.